HCCI Engine Combustion-Timing Control: Optimizing Gains and Fuel Consumption Via Extremum Seeking

Nick J. Killingsworth, *Member, IEEE*, Salvador M. Aceves, Daniel L. Flowers, Francisco Espinosa-Loza, and Miroslav Krstić, *Fellow, IEEE*

***Abstract*—Homogenous-charge-compression-ignition (HCCI) engines have the benefit of high efficiency with low emissions of NO_x and particulates. These benefits are due to the autoignition process of the dilute mixture of fuel and air during compression. However, because there is no direct-ignition trigger, control of ignition is inherently more difficult than in standard internal combustion engines. This difficulty necessitates that a feedback controller be used to keep the engine at a desired (efficient) setpoint in the face of disturbances. Because of the nonlinear autoignition process, the sensitivity of ignition changes with the operating point. Thus, gain scheduling is required to cover the entire operating range of the engine. Controller tuning can therefore be a time-intensive process. With the goal of reducing the time to tune the controller, we use extremum seeking (ES) to tune the parameters of various forms of combustion-timing controllers. In addition, in this paper, we demonstrate how ES can be used for the determination of an optimal combustion-timing setpoint on an experimental HCCI engine. The use of ES has the benefit of achieving both optimal setpoint (for maximizing the engine efficiency) and controller-parameter tuning tasks quickly.**

***Index Terms*—Extremum seeking (ES), homogenous-charge-compression-ignition (HCCI) engines, proportional-integral derivative (PID) tuning.**

I. Introduction

HOMOGENOUS-CHARGE-COMPRESSION-IGNITION (HCCI) engines have emerged as an efficient and low-polluting technology. This engine has attributes of both spark ignition (SI) and compression ignition (CI, "diesel") engines. HCCI engines utilize a premixed charge of fuel and air similar to SI engines. Different from SI engines, the HCCI fuel–air mixture is very dilute and ignited by compression. These characteristics allow HCCI engines to operate with higher compression ratios than SI engines, yielding higher efficiencies (similar to CI engines). Moreover, because the intake charge is dilute and premixed, the peak in-cylinder temperatures are significantly reduced, resulting in the formation of very little NO_x as compared to conventional SI and CI internal combustion engines [1].

While operation without a direct-ignition trigger yields an efficient and low-polluting engine, control of the combustion timing in HCCI engines is more difficult. Without a direct means of controlling the start of combustion, we must resort to actuating other engine parameters to indirectly control combustion. The rates at which chemical reactions proceed determine when the inducted fuel–air residual exhaust gas mixture will autoignite and depend on the gas temperature, pressure, and composition. Parameters that can be used to actuate combustion are as follows: gas temperature, density (pressure), composition, and mixture homogeneity [2]. In practice, the combustion timing can be managed by approaches such as the following: regulating the temperature of the intake charge [3], [4], retaining or reinducting hot residual gasses from the previous cycle [5]–[7], varying the compression ratio [7], [8], or by adding a more reactive secondary fuel [9].

Stable and efficient operation of HCCI engines requires that the combustion timing be tightly controlled to the proper setpoint. At high loads, early combustion can yield unacceptable pressure-rise rates $(\mathrm{d}p/\mathrm{d}\theta)$ or unacceptable peak cylinder pressure, causing excessive noise and potentially damage to the engine. Additionally, oxides of nitrogen (NO_x) tend to be higher as ignition advances [10]. On the other hand, late combustion timing leads to incomplete combustion and increases emissions of carbon monoxide (CO) and unburned hydrocarbons (UHC) [10], [11]. Combustion becomes unstable and can fail to occur (misfire) as the combustion timing is delayed further [10], [12]. Thus, the proper choice of the combustion timing at each operating point is crucial for HCCI engines.

Typically, a mapping procedure determines the combustion-timing setpoint for each operating point, defined by the speed and torque. Each operating point requires a sweep of the parameter space. The best values over this sweep populate a lookup table. While effective, this mapping procedure can be time-consuming. Popovic *et al.*[13] use a form of extremum seeking (ES) to speedup this process, finding that ES determines the same engine operating points as the standard mapping procedure in a fraction of the time. ES, a nonmodel-based optimization method, iteratively modifies the arguments (in this

Manuscript received February 12, 2008; revised June 25, 2008. Manuscript received in final form October 16, 2008. First published April 21, 2009; current version published October 23, 2009. This work was supported in part by the University of California Energy Institute, in part by the U.S. Department of Energy by Lawrence Livermore National Laboratory under Contract DE-AC52-07NA27344, in part by the National Science Foundation, and in part by Ford Motor Company. Recommended by Associate Editor Y. Jin.

N. J. Killingsworth, S. M. Aceves, D. L. Flowers, and F. Espinosa-Loza are with the Lawrence Livermore National Laboratory, Livermore, CA 94550 USA (e-mail: killingsworth2@llnl.gov; saceves@llnl.gov; flowers4@llnl.gov; espinosaloza1@llnl.gov).

M. Krstić is with the Cymer Center for Control Systems and Dynamics and Department of Mechanical and Aerospace Engineering, University of California, San Diego, La Jolla, CA 92093 USA (e-mail: krstic@ucsd.edu).

Digital Object Identifier 10.1109/TCST.2008.2008097

application, the engine parameters) of the cost function so that the output of the cost function reaches a local minimum or local maximum (as specified by the user). In this paper, we use a different form of ES [14] to find the combustion-timing setpoint that minimizes the fuel consumption of an experimental HCCI engine.

In addition to finding a stable and efficient combustion-timing setpoint, a controller is required to regulate the HCCI engine to this setpoint. Numerous HCCI engine combustion-timing control studies have successfully incorporated proportional-integral derivative (PID) controllers. Furthermore, a wide variety of actuation methods effectively work with PID control. Olsson *et al.* [9] incorporated gain-scheduled PID controllers to control the combustion timing of each cylinder of an experimental HCCI engine by regulating the octane number of the fuel mixture going to each cylinder. In the work by Haraldsson *et al.* [15], a novel variable-compression-ratio engine controls the mean combustion timing of all five cylinders using a PID controller.

In the study by Haraldsson *et al.* [4], a fast-thermal-management (FTM) actuation system controls the combustion timing. The FTM system consists of a stream of ambient air and a hot stream of air that passes through an exhaust heat exchanger; the two streams are mixed to regulate the intake air temperature. The FTM system controls the mean combustion timing of all the engine cylinders [4] and, later, the cylinder individual combustion timing [16]. PID controllers are used with gains that depend on the engine speed. Haraldsson *et al.* [4] find that changes in revolutions per minute alter the amount of heat transfer and, thus, the wall temperature.

Agrell *et al.*[7] used a PI controller with the combustion timing averaged over five cycles as the feedback signal and the valve timing on a single-cylinder engine with variable valve timing as the output. They used one of two different valve strategies dependent on the operating conditions: One changed the inlet-valve closing to vary the effective compression ratio and the other strategy used negative valve overlap, which traps more residual gas, increasing the temperature of the charge. In subsequent work, a feedforward controller was added to the PI controller [17]. The feedforward controller consists of an ignition model that is a nonlinear map covering a number of operating conditions and based on a knock integral [17].

Feedforward compensation was also used by Strandh *et al.* [18]. System identification was used to construct a model of the dual-fuel HCCI engine mentioned previously [9]. This model is used to derive a first-order feedforward filter. Comparing the performance of a PID controller with and without the feedforward filter, the feedforward filter increases the bandwidth of the controller, allowing cycle-by-cycle control.

In summary, PID controllers with and without feedforward compensation effectively control the combustion timing of various HCCI engines, using numerous options for actuation. However, PID controllers require the tuning of their parameters. Moreover, the nonlinear nature of HCCI engines requires gain scheduling to achieve good performance over the whole operating range of the engine, further increasing the task of tuning. There are many published methods available to tune PID controllers [19]. However, most tuning methods require a model of the system to be controlled. Physics-based models of HCCI engines tend to be overly complicated, and most system-identification approaches yield a linear model. Due to the nonlinear nature of HCCI engines, linear models are only valid near the operating point for which they are derived. Therefore, many linear models are required to span the operating range of an HCCI engine, which can be time intensive.

Nonmodel-based tuning methods are thus desirable. One such method is iterative feedback tuning (IFT). IFT iteratively optimizes the controller parameters with respect to a cost function derived from the output signal of the closed-loop system [20]. Recently, IFT was effectively applied to tune the combustion-timing control of an HCCI engine with variable valve timing [21]. However, tuning required two (three) experiments to be performed for each iteration for a 1 (2)-DOF controller. Thus, the tuning procedure is somewhat disjointed, and the controller parameters are calculated offline after these independent experiments are conducted.

In contrast to offline approaches, we present an online method for optimizing the step response of the combustion timing by tuning the HCCI engine controller. Specifically, we use a discrete version of ES [14] to minimize a cost function that quantifies the performance of the controller. The cost is a function of the error between the actual and desired combustion timing. The controller parameters are updated online as the optimization takes place. Thus, this method does not require offline calculations and greatly reduces the time to find optimal controller parameters. A previous study comparing ES PID tuning with other leading PID tuning methods on an assortment of simulated plants showed that ES PID tuning produced similar or better performance than the other tuning methods [22].

In the next section, we give a background of the ES algorithm used in this paper. We then describe the experimental HCCI engine system. Next, we present the use of ES to determine optimal combustion-timing setpoints on the experimental HCCI engine. Then, we outline the procedure for using ES for controller-parameter tuning and describe the form of the controller and the cost function used for combustion-timing control. Finally, we report the experimental combustion-timing controller tuning results.

II. ES

Typical control problems involve regulating the output of a system to a known setpoint. However, there are often cases where it is desirable to regulate the output to an optimal setpoint that is unknown or changing with time, where optimality is determined by the minimum or maximum of some cost function $J(\theta)$. These optimal setpoints are characterized by an extremum in the input–output map; a map that is often nonlinear. For such cases, ES, a nonmodel-based online optimization method, can be used to find the unknown optimal setpoint [14]. In a similar manner, ES is a powerful tool for determining optimal system parameters or control gains.

ES is a gradient-based optimization method. ES differs from standard gradient-based optimization algorithms in the manner it obtains the gradient information. Standard gradient-based optimization methods require that the gradient is known, whereas ES does not require any information about the gradient or map.

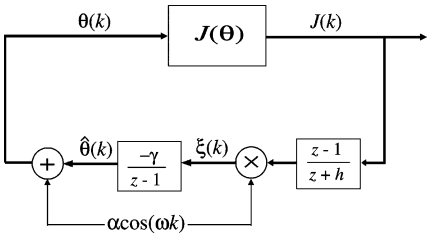

Fig. 1. Discrete ES scheme. The input parameters $\theta(k)$ are perturbed by the signal $\alpha_i \cos(\omega_i k)$. The output of the cost function $J(\theta(k))$ is then high-pass filtered, demodulated, and finally low-pass filtered to yield new input parameters $\hat{\theta}(k)$. After successive steps k, $\hat{\theta}(k)$ approaches θ^*, the minimizer of $J(\theta(k))$.

However, because ES is a gradient method, the input θ found by ES is not necessarily a global minimizer of $J(\theta)$.

As shown in Fig. 1, ES achieves optimization by sinusoidally perturbing the input parameters $\theta(k)$ of the system and, then, estimating the gradient $\nabla J(\theta(k))$ caused by the perturbation, where k is the index of the ES algorithm. To determine the gradient, we first high-pass filtered the cost-function signal $J(\theta(k))$ to remove the slow portion of the signal and, then, demodulated the output by multiplication with a sinusoidal signal of the same frequency as the perturbation signal. This procedure estimates the gradient by picking off the portion of the cost-function signal $J(\theta(k))$ that arises due to perturbation of the input signal. We then use the gradient information to modify the input parameters in the next iteration. Specifically, the gradient estimate is integrated, yielding a new parameter estimate $\hat{\theta}(k)$. The integrator performs both the adaptation function and acts as a low-pass filter.

The time-domain implementation of the discrete-time ES algorithm in Fig. 1 is

$$\zeta(k) = -h\zeta(k-1) + J(\theta(k-1)) \tag{1}$$

$$\hat{\theta}_i(k+1) = \hat{\theta}_i(k) - \gamma_i \alpha_i \cos(\omega_i k) \times [J(\theta(k)) - (1+h)\zeta(k)] \tag{2}$$

$$\theta_i(k+1) = \hat{\theta}_i(k+1) + \alpha_i \cos(\omega_i(k+1)) \tag{3}$$

where $\zeta(k)$ is a scalar and the subscript i indicates the ith entry of a vector. γ_i is the adaptation gain, and α_i is the perturbation amplitude. Stability and convergence are influenced by the values of γ, α, and the shape of the cost function $J(\theta)$ near the minimizer. The perturbation frequency ω_i should be high relative to the timescale of the ES dynamics in discrete time, which is primarily governed by the adaptation gain. It is important that each ω_i frequency is distinct. We choose the modulation frequency ω_i such that $\omega_i = a^i \pi$, where a satisfies $0 < a < 1$. Additionally, we design the high-pass filter $(z-1)/(z+h)$ with $0 < h < 1$ and a cutoff frequency well below the modulation frequencyω_i.

The complete proof of stability is presented in [23] and is based on two-timescale averaging [24] for the system

$$\tilde{\theta}(k+1) = \tilde{\theta}_k + \gamma\alpha\cos(\omega k) \times \left(e + \frac{J''}{2}\left(\tilde{\theta} - \alpha\cos(\omega k)\right)^2\right) \tag{4}$$

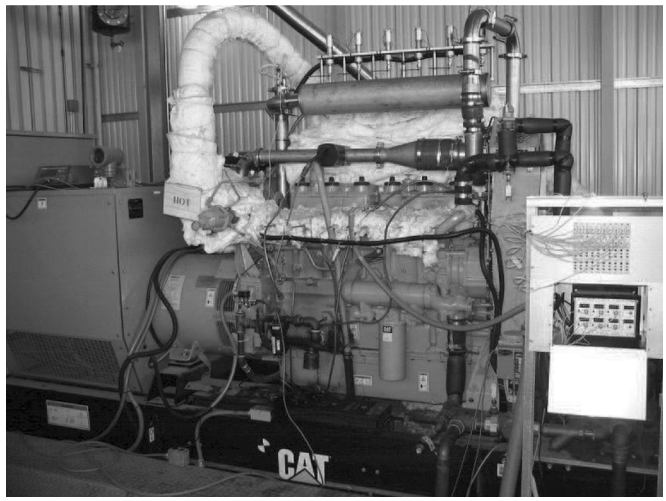

Fig. 2. HCCI engine used in these experiments: 14.6-L six-cylinder natural-gas engine setup for stationary power generation.

$$e(k+1) = -he(k) - (1+h)\frac{J''}{2} \times \left(\tilde{\theta} - \alpha\cos(\omega k)\right)^2 \tag{5}$$

where $e = J^* - (1+h)/(z+h)$[J], with the assumption thatγ and α are small. The proof guarantees exponential convergence of $J(\theta(k))$ to $J^* + O(\alpha^3)$.

ES is a local optimization method, but the prospects for reaching a global extremum increase with the size of the perturbation amplitude. This point was studied in the work of Tan *et al.* [25]. The obvious tradeoff is that, with increasing of the perturbation amplitude, the improved prospects of converging to a vicinity of a global extremum is accompanied with the increased residual oscillation. This problem can be somewhat remedied by making the perturbation amplitude dependent on the value of the cost. For example, in minimization problems, one would make the perturbation amplitude a monotonically increasing function of the value of the cost $J(\theta(k))$. This ensures that the residual oscillation is small when the cost has become so small that its further decrease toward the "global" minimum would yield very little reduction of the cost. This idea was successfully pursued in the application to beam matching in charged-particle accelerators in [26].

III. Experimental Setup

A 14.6-L Caterpillar 3406 natural-gas SI engine converted to run in HCCI mode [27] is used in this paper. Fig. 2 shows a picture of the engine and Table I lists major engine parameters. The fueling system consists of a carburetor coupled to an electronic natural-gas pressure-control valve, allowing for adjustment of the fuel–air equivalence ratio ($\sim$0.3–0.4). A turbocharger provides intake pressure boost, which is further augmented by a custom centrifugal supercharger. An electronically controlled throttle valve regulates the engine speed by restricting the air flow into the engine.

A thermal-management system shown in Fig. 3 controls the combustion timing of the engine on a cylinder-by-cylinder

TABLE I
CATERPILLAR 3406 ENGINE PARAMETERS

number of cylinders	6
total displacement	14.6 L
compression ratio	16:1
cylinder bore	137 mm
connecting rod length	330 mm
stroke	164 mm

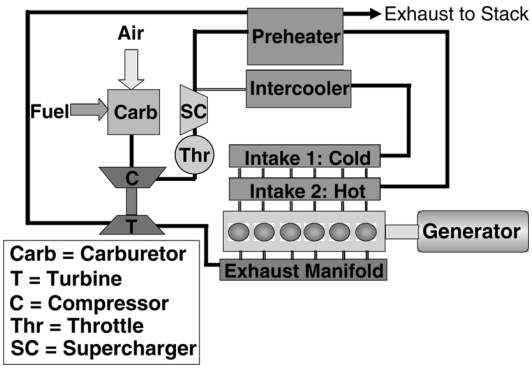

Fig. 3. Schematic of the experimental HCCI engine thermal-management system. On each cylinder, a valve regulates the blend of hot and cold fuel–air mixture, controlling the intake temperature.

basis. The thermal-management system controls the temperature of gases inducted into each cylinder, which in turn controls the autoignition process. Inducted air flows through the carburetor where fuel is added, then travels through the turbocharger, throttle, and supercharger. Then, after the supercharger, the fuel–air mixture splits into two streams, one "hot" and one "cold." The hot side passes through an exhaust-to-intake heat exchanger, while the cold side travels through an aftercooler. The hot and cold streams are delivered to two separate manifolds. Each cylinder has a temperature-mixing valve where cold intake charge is blended with the charge from the hot manifold, regulating intake temperature to each cylinder. Each temperature-control valve is computer controlled using an electric servomotor. The length of the intake runners results in about a one-cycle transport delay before a change in the valve input affects the intake mixture entering the cylinder. This thermal-management system allows the intake temperature of each cylinder to be quickly adjusted for cylinder-by-cylinder control of the combustion timing.

The combustion-timing feedback signal is derived from in-cylinder measurements of the pressure. A camshaft-encoder hardware triggers acquisition from a pressure transducer every 0.5 crank-angle degrees (CAD). A net-heat-release analysis of the pressure measurements determines the combustion timing in each cylinder [28]. Specifically, we define the combustion timing to be the crank angle at which 50% of the heat has been released (CA50). Finally, the calculated combustion timing is used as a feedback, allowing control of the combustion timing by means of the temperature-control valves. Labview-based software handles all data acquisition and control tasks. The time-critical portions of the control software reside on a dedicated desktop PC running Labview Real-Time.

IV. FUEL-CONSUMPTION MINIMIZATION

For a given operating point defined by the speed and torque requirements of the engine, there is a combustion timing that minimizes the fuel consumption. This optimal combustion timing balances the work extracted from the combusting gases, heat-transfer losses, and combustion efficiency. When combustion begins before the piston reaches top dead center (TDC), expansion of the hot combusting gases combined with decreasing cylinder volume results in high pressure and temperature, impeding the piston motion. Additionally, the high temperature leads to an increase in NO_x, and even engine damage is possible if the pressure is too high. Furthermore, as the combustion timing advances, there is more time for heat transfer. Conversely, as the combustion is retarded to after TDC, the peak cylinder pressure and temperature are reduced due to the motion of the retreating piston, and the gas performs less work. At late timing, the reduction in temperature and pressure can lead to incomplete combustion. Therefore, some of the fuel's chemical energy fails to be released and is transported out the exhaust valve as UHC and CO. For each operating point, there is an optimal combustion timing that is a compromise between all these effects.

The optimal combustion timing is difficult to predict due to the numerous competing processes and must be experimentally determined. A mapping procedure is typically used to find the optimal combustion timing in standard internal combustion engines. At each operating point, a range of spark or injection timings are swept for SI and CI engines, respectively. The optimal combustion timing is then determined from the mapping data. However, this mapping procedure can be time consuming. ES can be a useful tool to speedup this process; it is well suited for finding unknown setpoints that optimize a nonlinear performance metric. In this paper, we use the engine's fuel consumption as the performance metric and ES to determine the combustion-timing setpoint that minimizes it.

To minimize the engine's fuel consumption, we use a cost function within ES that consists of the fuel consumption averaged over 100 engine cycles

$$J_{\text{fuel}}(\theta) \triangleq \frac{1}{n_f - n_0} \left(\sum_{n=n_0}^{n_f} \dot{m}_{\text{fuel}}(n, \theta) \right) \tag{6}$$

where n is the engine cycle, $\dot{m}_{\text{fuel}}(n, \theta)$ is the mass flow rate of fuel into the engine in grams per second, and θ is the combustion-timing setpoint. Therefore, in this case, the input parameter for the cost function (and parameter adjusted by ES) is defined as the 50% burn-location setpoint $\theta \triangleq \text{CA50}_{\text{setpoint}}$. The cost function $J_{\text{fuel}}(\theta)$ defined in (6) takes into account the fuel consumption over the interval $[n_0, n_f]$ after a delay of 200 engine cycles. Therefore, ES executes every 300 engine cycles, and the cost is evaluated for the last 100 cycles to allow the controller to get the engine to the new combustion-timing setpoint. A PID controller is used to regulate the measured 50% burn location $\text{CA50}_{\text{measured}}$ to the setpoint and is described in more detail in Section V.

The ES parameters were picked following the guidelines presented in Section II. The perturbation amplitude α_i is chosen as a small percentage of the input θ, and its optimal value depends

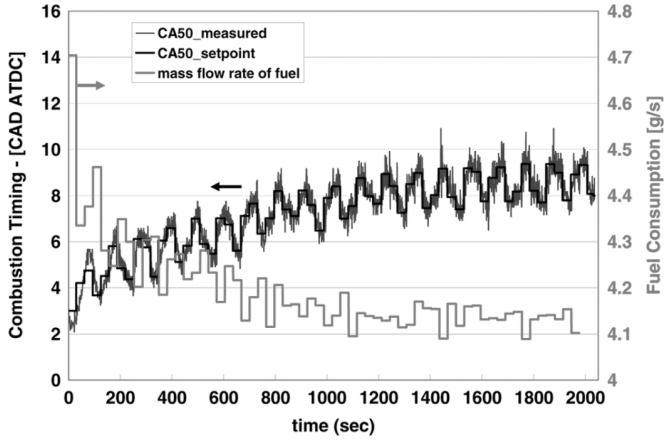

Fig. 4. Using conservative parameters, ES minimizes the fuel consumption by retarding the combustion timing from 3 to 8 CAD ATDC.

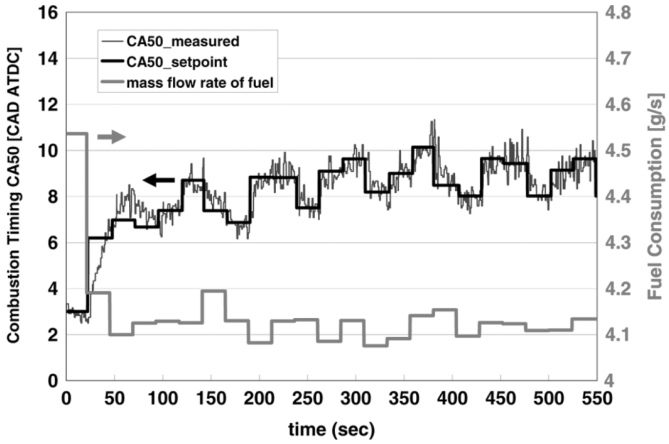

Fig. 5. Using more aggressive parameters, ES minimizes the fuel consumption by retarding the combustion timing from 3 to 8 CAD ATDC more quickly.

on the sensitivity of the cost function to changes in the input. The choice of adaptive gain γ is highly dependent on the response of the cost function to changes in the input and, therefore, the perturbation amplitude α_i. A safe method is to start with a small value of γ and increase it until ES seems to be adapting at an acceptable rate without becoming unstable.

ES was applied to the experimental HCCI engine running at 1500 r/min. Note the load and revolution per minute are held constant during tuning of the optimal combustion-timing setpoint. The combustion-timing setpoint, the solid black line shown in Fig. 4, is adjusted by ES every 300 engine cycles. This figure shows that ES delays the combustion-timing setpoint to just after 8 CAD after TDC (ATDC) from an initial combustion timing of 3 CAD ATDC. As the combustion timing is delayed, the fuel consumption is reduced; as shown on the right vertical axis in Fig. 4.

The optimization process took around 50 iterations (about 30 min). The experiment was repeated in Fig. 5 at the same operating point as in Fig. 4 but with a larger value of the adaptation gain γ. ES finds the same minimum but much more quickly ($\sim$10 min) with the larger gain. The total optimization time is also highly dependent on the wait time n_0 and the the total number of cycles evaluated $n_f - n_0$ in the cost function. As these parameters are reduced, the amount of time each iteration of ES takes is shorter.

An important next step would be to consider emissions in the optimization, and this could easily be done by including real-time emission measurements in the cost function (6) in addition to the fuel consumption. However, the authors did not have access to such equipment and, thus, did not include emission measurements.

V. Combustion-Timing Controller Tuning

In this section, we will use ES to tune the combustion-timing controller on the experimental engine of Section III. The controller-parameter tuning occurs online (while the engine is running) such that a cost function is minimized. First, we will describe the form of the combustion-timing controller. We use a PID controller, which compares the difference between the desired combustion-timing setpoint $\mathrm{CA50_{sp}}$ and the measured combustion timing $\mathrm{CA50}_m$ of the HCCI engine and produces a control signal $u(t)$ to reduce the difference between them. Specifically, $u(t)$ is the temperature-control-valve position and, thus, determines the intake temperature for each cylinder.

We use a standard PID controller with the exception that the derivative term acts on the measured output but not on the reference signal avoiding large control effort during a step change in the reference signal. We also investigate adding a feedforward term K_f to the PID controller. The form of the controller is

$$u(t) = K_f r(t) + K\left(e(t) + \frac{1}{T_i}\int_0^t e(\tau)\mathrm{d}\tau - T_d\frac{\mathrm{d}y(t)}{\mathrm{d}t}\right) \tag{7}$$

where the error $e(t) \triangleq r(t) - y(t)$ is the difference between the reference $r(t)$ and the measured output $y(t)$ signals of the closed-loop system. The Laplace transforms of the feedforward $C_r(s)$ and feedback $C_y(s)$ portions of the controller are

$$C_r(s) = K_f + K\left(1 + \frac{1}{T_i s}\right) \tag{8}$$

$$C_y(s) = K\left(1 + \frac{1}{T_i s} + T_d s\right). \tag{9}$$

A. Cost Function

ES tunes the parameters of the combustion-timing controller to minimize a given cost function. The cost function quantifies the performance of the controller; specifically, the controller's ability to track a square-wave reference signal. We use a cost function based on the integrated squared error

$$J(\theta) \triangleq \frac{1}{N}\left(\sum_{n=n_0}^{n_f} \mathrm{e}^2(n,\theta) + \sum_{n=n_0+\delta}^{n_f+\delta} \mathrm{e}^2(n,\theta)\right) \tag{10}$$

where n is the engine cycle, N is the total number of engine cycles evaluated, δ is the period of the square-wave reference signal, and θ contains the controller parameters

$$\theta \triangleq [K_f, K, T_i, T_d]^{\mathrm{T}}. \tag{11}$$

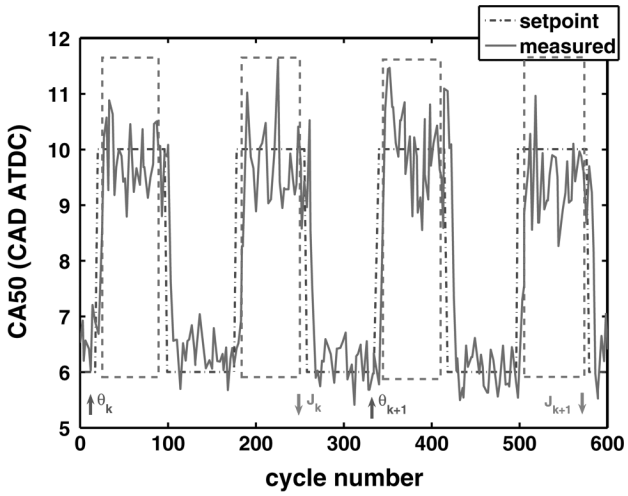

Fig. 6. Timing of ES PID tuning scheme. The cost function J is calculated every two periods of the square-wave reference signal. Additionally, the cost function is evaluated only at the later combustion timing as indicated by the dashed red box. The new PID parameters $\theta(k+1)$ are updated every two periods and after the cost $J(\theta(k))$ is calculated.

The cost function $J(\theta)$ defined in (10) accounts for the tracking error over the interval $[n_0, n_f]$ for two successive periods δ of the square-wave reference signal. By setting n_0 to approximate the engine cycle n_{peak} at which the step response of the closed-loop system reaches the first peak or maximum, the cost function $J(\theta)$ places zero weighting on the initial transient portion of the response [29]. Hence, the controller is tuned to minimize the error beyond n_{peak}, ignoring the initial transient.

Fig. 6 shows an example of how the cost function $J(\theta(k))$ is evaluated in the experiment. The calculation of the cost uses only the data points within the dashed box. We evaluate the cost only at the later combustion timing. Thus, for a step from 6 to 10 CAD ATDC, the cost is evaluated only for operation at 10 CAD ATDC. The sensitivity of the combustion timing becomes greater as combustion is delayed [10], [30]. Therefore, an optimal controller for going from $\text{CA50} = 6$ to 10 CAD ATDC will be stable during the transition from 10 to 6 CAD ATDC, whereas the opposite case will not necessarily result in stable operation. The cost is generated after two periods of the square wave, shown in Fig. 6 with the downward-pointing arrows.

The cost function must have a sufficient signal-to-noise ratio such that ES can resolve the effect of the perturbation signal $\alpha_i \cos(\omega_i k)$. Evaluating the cost over two periods of the reference signal, rather than one, reduces the variance, allowing the tracking behavior of the current controller to be seen more clearly. Additionally, to help isolate the effect of the current controller, we low-pass filtered the measured combustion-timing signal evaluated in the cost function. The plots, however, present the unfiltered combustion-timing signal.

B. Experimental Controller Tuning

Fig. 7 shows the overall ES PID tuning scheme. The ES algorithm uses the value of the cost function at iteration k to compute new controller parameters for the next iteration $k+1$, as shown in Fig. 6. The new controller is applied during the next two periods of the square-wave reference signal. The process continues iteratively.

The combustion-timing controller for cylinder one receives a square-wave combustion-timing reference signal. While all the other cylinders have a fixed combustion timing in an effort to keep the engine speed constant (changing the combustion timing produces a small change in the torque produced as is discussed in Section IV and can cause a disturbance in the engine speed). The one per-revolution pulse from the camshaft encoder provides the timing signal for the square-wave reference signal, which has a period of 160 engine cycles. Starting with a stable and conservative controller, we run at least four periods of the reference signal to generate initial conditions for the ES algorithm.

The engine was run at 1600 r/min with a load of 25 kW. For each period of the square-wave reference signal, the cost is evaluated from $n_0 = 10$ to $n_f = 70$ engine cycles, and for every experiment, the parameters a and h in the ES scheme (1), (2), and (3) are set to 0.7 and 0.5, respectively.

Fig. 8 shows the ES tuning of a PI controller ($T_d = K_f = 0$). The initial PI controller is parameterized with $\theta = [0, 1, 0.1, 0]^{\text{T}}$ defined in (11). The ES perturbation frequency is $\omega = \pi[0, a^2, a, 0]^{\text{T}}$. Because $0 < a < 1$, the perturbation frequency of the integral time T_i is higher than for proportional gain K. Fig. 8 shows the combustion-timing (CA50) setpoint and the measured combustion timing. With the initial (untuned) controller parameters, the PI controller is unable to regulate the combustion timing to the setpoint within a period of the square-wave reference signal as shown in Fig. 8(a). However, as ES tunes the controller parameters, the controller is able to adjust the engine's inlet temperature fast enough to move from $\text{CA50} = 6$ to 10 and back to 6 within 160 engine cycles, see Fig. 8(b). Greater overshoot occurs as the controller becomes better tuned. This overshoot is because the natural variability in the ignition process is more pronounced at later combustion timings, which the improved controller is better able to achieve. This phenomenon can be seen in greater detail in Fig. 8(b).

In this experiment, the perturbation amplitude α and adaptive gain γ are conservative, and thus, ES slowly reduces the cost function $J(\theta)$ by reducing the integral time T_i and by increasing the proportional gain K. These changes increase the effect of both the proportional and integral terms of the controller. For this case, the tuning algorithm converges in approximately 125 iterations of ES or 50 min. A better choice of the initial controller parameters will reduce the tuning time, because the initial parameters will likely be closer to the optimal parameters requiring less adjustment; additionally, the controller will be able to track a step change in the combustion timing more precisely so a shorter period of the reference signal can be used. It would also be possible to decrease the tuning time by reducing the number of samples N evaluated in the cost function $J(\theta(k))$ as the cost becomes smaller. The minimum cost and the minimizer θ^* are listed in Table II. Note that the perturbation amplitude α was reduced while the experiments were running, particularly as the integral time T_i became smaller.

The derivative term was included in the tuning shown in Fig. 9 with a perturbation frequency $\omega = \pi[0, a^2, a, a^3]^{\text{T}}$.

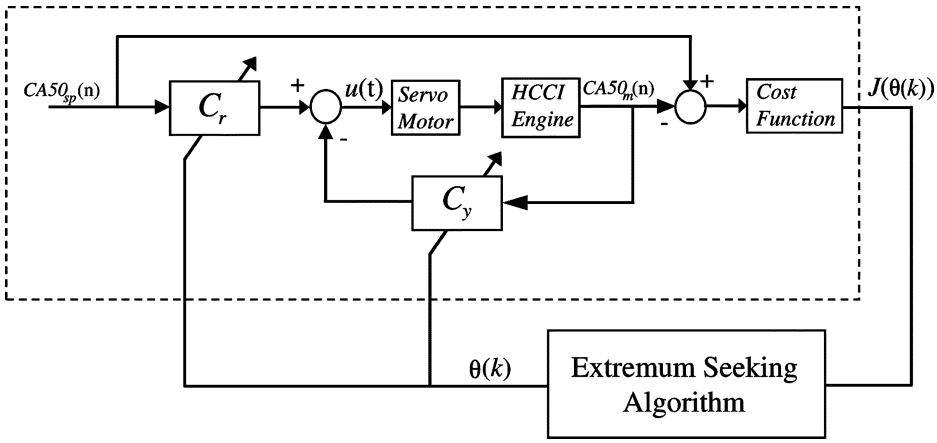

Fig. 7. Overall ES PID tuning scheme including the dynamics of the temperature-control valves and HCCI engine. The ES algorithm updates the controller parameters $\theta(k)$ to minimize the cost function $J(\theta)$, which is calculated from the response of the combustion-timing controller to a square-wave reference signal during continuous operation of the HCCI engine shown within the dashed box.

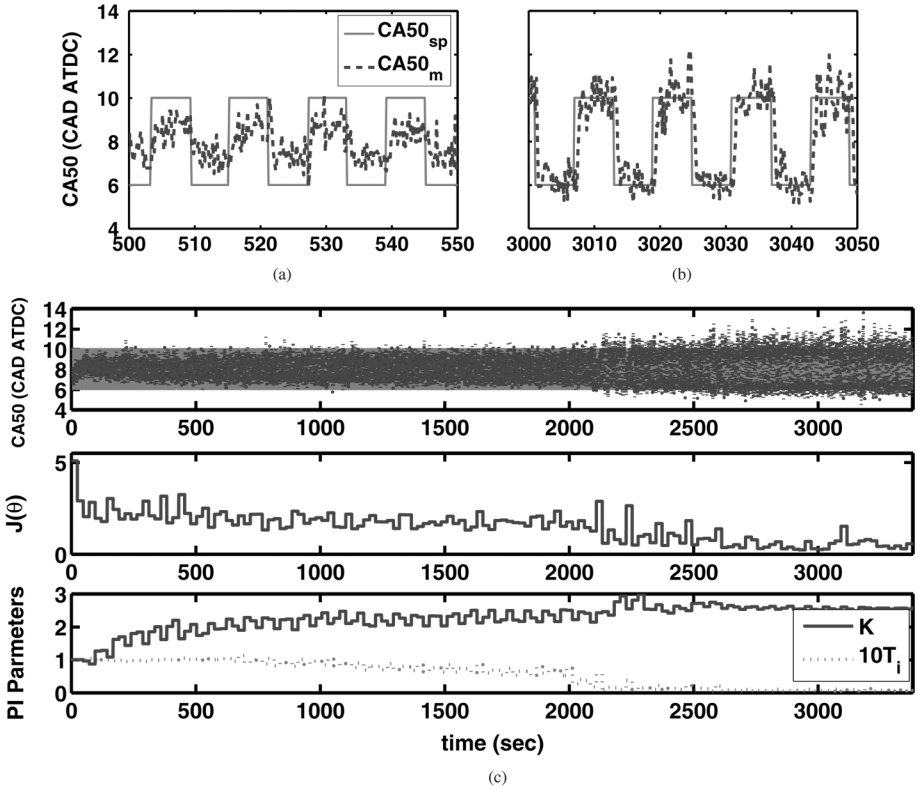

Fig. 8. ES tuning of PI controller. (a) Tracking of the desired combustion-timing setpoint CA50sp at the beginning of the tuning process. (b) Improved tracking at the end. The entire tuning process is illustrated in (c) with the top plot showing tracking, the middle plot shows the evolution of the cost function, and the third plot shows the PI parameters during tuning.

TABLE II
ES CONTROLLER TUNING RESULTS

Controller	Cost	K_f	K	T_i	T_d
PI (Fig. 8)	0.222	0	2.53	0.00500	0
PID (Fig. 9)	0.222	0	2.01	0.00501	0.00327
PI + FF (Fig. 10)	0.0965	3.56	0.942	0.114	0
PI + FF (Fig. 11)	0.0465	3.43	0.161	0.0333	0
PI + FF (Fig. 12)	0.265	1.26	0.923	0.00300	0

The initial PID controller consists of the parameters $\theta = [0, 1, 0.08, 0.005]^{\mathrm{T}}$. Similar to the previous experiment, ES increases the proportional gain K while decreasing the integral time T_i. Additionally, the derivative time T_d is decreased. Results in Table II show that the PID controller found using ES produces an identical minimum cost as was found with the PI controller. However, it should be noted that, for these experiments, the reference signal oscillates between 8 and 11 CAD ATDC rather than the 6 and 10 CAD ATDC used for the PI tuning shown in Fig. 8, so direct comparison of their costs cannot be made. The results in Table II show that ES finds a small value of the derivative time T_d, so it appears that, at this operating point, the addition of the derivative term does not play a key role. Note that the PID parameters converge in around

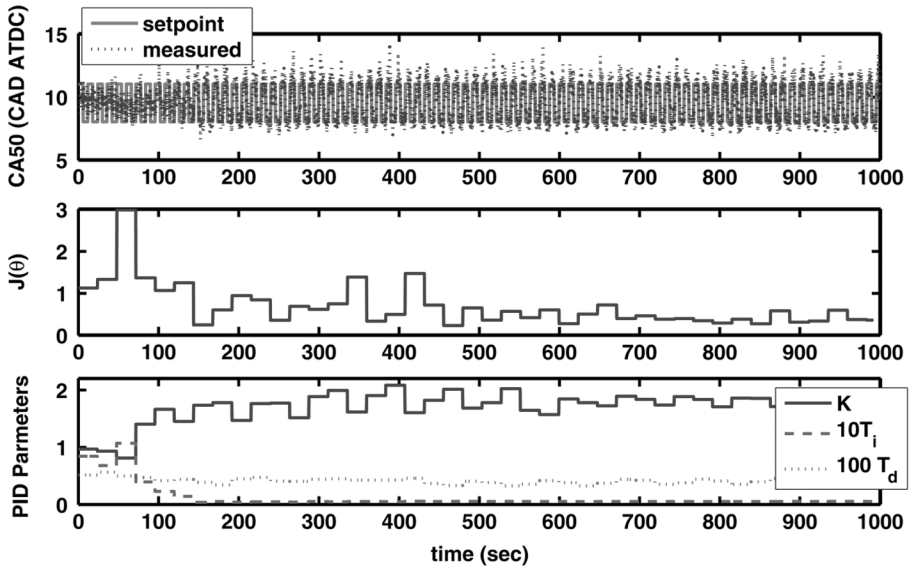

Fig. 9. ES tuning of PID controller illustrated by tracking of the combustion timing with a square-wave reference signal, evolution of the cost function, and the PID parameters during tuning.

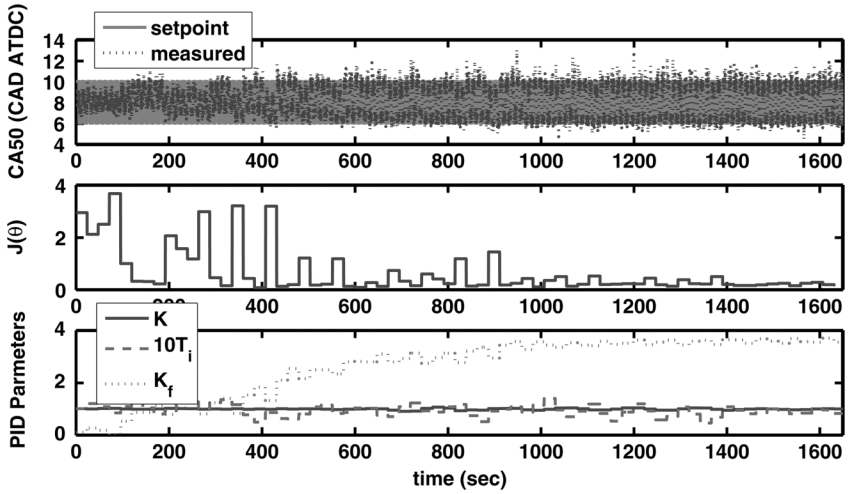

Fig. 10. ES tuning of PI plus feedforward controller illustrated by tracking of the combustion timing with a square-wave reference signal, evolution of the cost function, and the PI and feedforward parameters during tuning.

15 min for this case. This decreased tuning time is because larger values of the perturbation amplitude α and adaptive gain γ were used. Typically, increasing α and γ will increase the speed of convergence. However, when these parameters are too large, the stability of ES can be affected [22].

Next, we look at tuning an additional constant feedforward term K_f. The initial controller used is $\theta = [0.1, 1, 0.1, 0]^{\mathrm{T}}$, and the ES perturbation frequency is $\omega = \pi[a, a^3, a^2, 0]^{\mathrm{T}}$. Fig. 10 shows that, in this case, the feedforward term is quickly increased, while the other parameters stay relatively constant. Initially, the cost function fluctuates from a high value to a low value. This behavior occurs because the measured combustion timing does not track the reference signal well. The combustion timing becomes delayed occasionally and tracks the later part of the reference signal resulting in a lower cost, but then, it becomes advanced and the cost goes up. Using a longer reference signal period δ will reduce this effect but at the expense of longer tuning times. Another solution to minimize the artificial fluctuation in the cost function would be to also include the tracking error during the earlier combustion timing in the cost.

Fig. 11 shows a repeat of the experimental conditions from the previous run, but this time, ES finds a different local minimizer. Table II shows that a similar feedforward term K_f is found. However, both the proportional gain K and the integral time T_i are reduced. While the proportional gain is almost an order of magnitude smaller in this experiment versus the previous one, the integral gain $K_i = (K)/(T_i)$ is 4.83 for this experiment and 8.28 for the previous experiment. Thus, the integral gains for the two different controllers are closer in magnitude than the proportional gains. In addition, notice that the reduction in the feedback controller gains K and K_i results in a reduced cost in Table II for this controller.

Fig. 12 shows another run of ES tuning of a PI plus feedforward controller. This experiment is identical to the past two

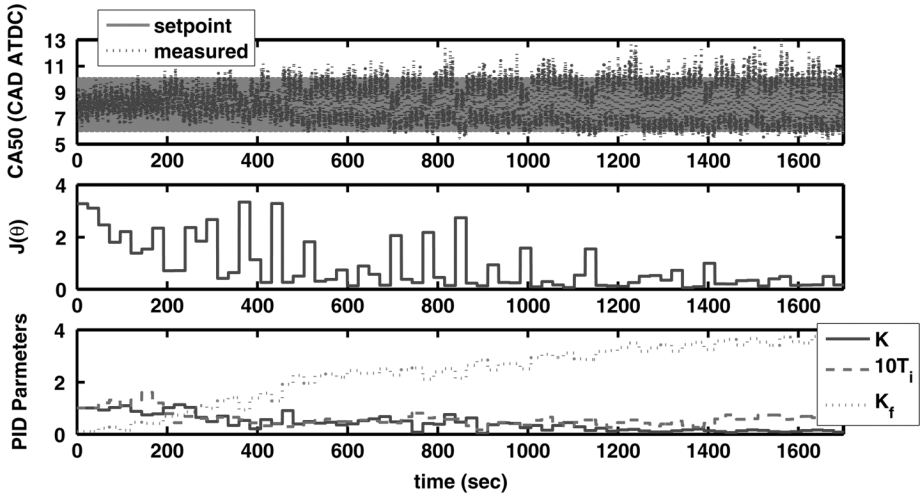

Fig. 11. Repeat of ES tuning of PI plus feedforward controller (Fig. 10) illustrated by tracking of the combustion timing with a square-wave reference signal, evolution of the cost function, and the PI and feedforward parameters during tuning.

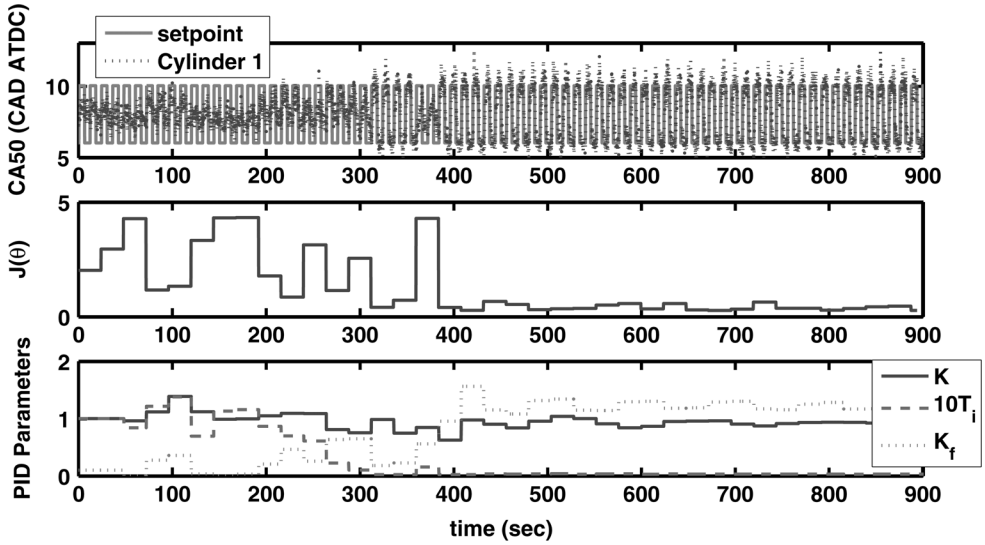

Fig. 12. Repeat of ES tuning of PI plus feedforward controller with alternate perturbation frequency illustrated by tracking of the combustion timing with a square-wave reference signal, evolution of the cost function, and the PI and feedforward parameters during tuning.

experiments shown, with the exception of the perturbation frequency. The ES perturbation frequency is $\omega = \pi[a^2, a^3, a, 0]^{\mathrm{T}}$; therefore, the integral time T_i receives the highest frequency rather than the feedforward term K_f. The change in perturbation frequency results in the integral time T_i changing more quickly and the discovery of a new local minimizer. The role of the feedforward gain K_f is reduced, and the integral gain plays a more dominant role in the setpoint response of the controller. Figs. 10, 11, and 12 show that there are multiple local minimizers of $J(\theta)$ and that either the feedforward term K_f or integral gain K_i can play a dominant role in the setpoint response. However, a large integral gain results in a larger high frequency gain and affects the steady-state response. Therefore, a local minimizer with a large integral gain K_i tends to have a higher cost. We can see from these experiments the influence of picking the perturbation frequency for each parameter in θ. The input parameter with the highest frequency will be perturbed more often than the other input parameters, and assuming a gradient $\nabla J(\theta(k))$ is generated because of the perturbation, this input parameter will also be modified more often. In short, the choice of perturbation frequency affects how ES navigates the controller-parameter space. Because of the appearance of local minima, the operator might want to rerun the tuning procedure starting from a new initial condition and pick the controller parameters that result in the lowest cost.

C. Disturbance Rejection

The formulation of the square-wave reference signal and the cost function (10) used for ES tuning emphasizes the controller's setpoint response. The setpoint response of the combustion-timing controller is important during the transition between low and high loads because these conditions require different combustion timings. At low loads, an early combustion timing will be desirable to minimize CO and UHC emissions, whereas at higher loads, a later combustion timing will minimize NO_x and the pressure rise rate. Furthermore, the

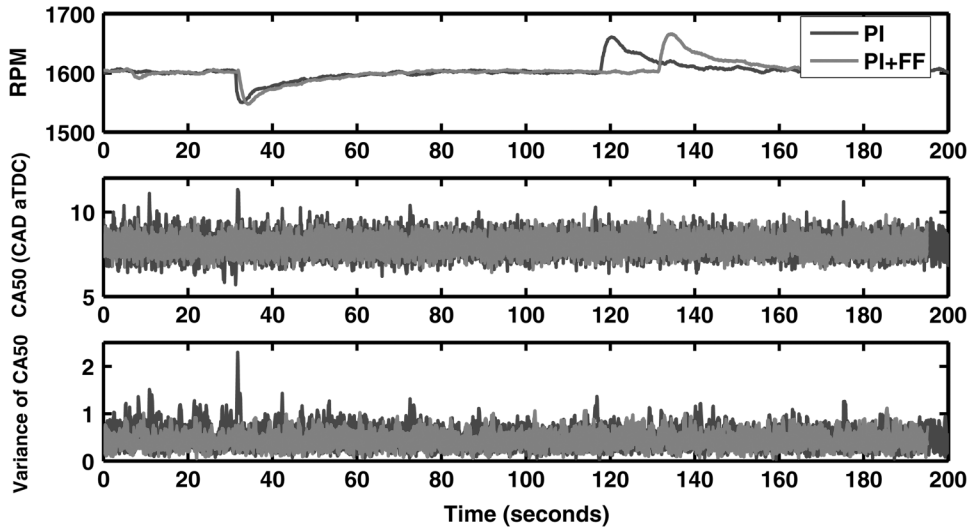

Fig. 13. Load disturbance with PI and PI plus feedforward combustion timing controllers. The plots present the revolution per minute, tracking of the CA50 $\text{setpoint} = 8$ CAD ATDC, and the standard deviation of combustion timing during load disturbance.

combustion timing that yields the maximum brake torque will change with load and speed.

However, the disturbance rejection of the controller is also important during speed and load transients. This fact makes a case for using a controller with feedforward compensation. The feedforward term can be used to handle the setpoint changes, while the feedback portion need not be so aggressive and can better deal with disturbance rejection.

Disturbance rejection will now be studied to test the versatility of PI versus PI plus feedforward controllers. Two separate experiments are shown in Fig. 13, one with a PI controller and the other with a PI plus feedforward controller. In both experiments, the CA50 setpoint is held constant at 8 CAD ATDC, while the load is changed from 21 to 25 kW and back to 21 kW. The load change can be seen in the revolution per minute. As the load is increased, the revolution per minute falls off; inversely, as the load is decreased, the revolution per minute increases. In Fig. 13, the PI controller found in the experiment shown in Fig. 8 is compared to the PI plus feedforward controller from Fig. 12. In this plot, we can see that the use of the feedforward term allows the feedback part of the controller to better reject disturbances. The measured combustion timing differs from the setpoint by more than 2 CAD at times when the PI controller is used. In addition, when the PI controller is used, the standard deviation exceeds one particularly after the load changed. In contrast, the PI plus feedforward controller keeps the combustion timing well within ± 2 CAD of the setpoint and the standard deviation less than one.

VI. Conclusion

ES tuning is an effective method to tune PI, PI plus feedforward, and PID controllers and does so in a timely fashion. The PI plus feedforward controller provides good setpoint response in addition to disturbance rejection when compared with a PI controller. Gain scheduling is needed for HCCI controllers; ES can effectively populate the controller parameters for gain scheduling to span the loads and speeds that define an engine's operating range.

Additionally, ES has been shown to be a fast and effective method to map an HCCI engine. ES was used to determine the combustion timing that yields the minimal fuel consumption. In the case of engines that undergo slow transients during operation, ES can be used to continually provide the optimal input parameters. This method could therefore be used on stationary engine/generator sets to minimize fuel consumption dynamically during operation.

A possible extension of this paper would be to combine the setpoint optimization of Section IV with controller tuning of Section V. These two ES loops could work simultaneously with proper separation of timescales. The loop for selecting the optimal controller parameters should be fast with respect to the ES loop for finding the optimal setpoint.

Acknowledgment

The authors would like to thank T. Ross for helping operate the experimental engine.

References

[1] S. M. Aceves, D. L. Flowers, J. Martinez-Frias, J. R. Smith, R. Dibble, M. Au, and J. Girard, "HCCI combustion: Analysis and experiments," presented at the SAE Government Industry Meeting Expo., Washington, DC, 2001, SAE Paper 2001-01-2077.

[2] J. Yang, T. Culp, and T. Kenney, "Development of a gasoline engine system using HCCI technology—The concept and test results," presented at the SAE Powertrain & Fluid Systems Conf. & Exhibition, San Diego, CA, 2002, SAE Paper 2002-01-2832.

[3] J. Martinez-Frias, S. M. Aceves, D. L. Flowers, J. R. Smith, and R. Dibble, "HCCI engine control by thermal management," presented at the Int. Fuels & Lubricants Meeting & Expo., Baltimore, MD, 2000, SAE Paper 2000-01-2869.

[4] G. Haraldsson, J. Hyvönen, P. Tunestål, and B. Johansson, "HCCI closed-loop combustion control using fast thermal management," presented at the SAE 2004 World Congr. & Exhibition, Detroit, MI, 2004, SAE Paper 2004-01-0943.

[5] G. M. Shaver and J. C. Gerdes, "Cycle-to-cycle control of HCCI engines," in *Proc. ASME Int. Mech. Eng. Congr. Expo.*, Washington, DC, 2003, IMECE2003-41966.

[6] C. J. Chiang and A. G. Stefanopoulou, "Control of thermal ignition in gasoline engines," in *Proc. Amer. Control Conf.*, Portland, OR, 2005, pp. 3847–3852.
[7] F. Agrell, H. E. Ångstrom, B. Eriksson, J. Wikander, and J. Linderyd, "Integrated simulation and engine test of closed-loop HCCI control by aid of variable valve timings," presented at the SAE 2003 World Congr. & Exhibition, Detroit, MI, 2003, SAE Paper 2003-01-0748.
[8] G. Haraldsson, J. Hyvönen, P. Tunestål, and B. Johansson, "HCCI combustion phasing in a multi cylinder engine using variable compression ratio," presented at the SAE Powertrain & Fluid Syst. Conf., San Diego, CA, 2002, SAE Paper 2002-01-2858.
[9] J. Olsson, P. Tunestål, and B. Johansson, "Closed-loop control of an HCCI engine," presented at the SAE 2001 World Congr., Detroit, MI, 2001, SAE Paper 2001-01-1031.
[10] J. Olsson, P. Tunestål, B. Johansson, S. Fiveland, R. Agama, M. Willi, and D. Assanis, "Compression ratio influence on maximum load of a natural gas fueled HCCI engine," presented at the SAE 2001 World Congr., Detroit, MI, 2002, SAE Paper 2002-01-0111.
[11] S. M. Aceves, D. L. Flowers, J. Martinez-Frias, F. Espinosa-Loza, M. Christensen, B. Johansson, and R. P. Hessel, "Analysis of the effect of geometry-generated turbulence on HCCI combustion by multi-zone modeling," presented at the SAE Brasil Fuels & Lubricants Meeting, Rio De Janiero, Brazil, 2005, SAE Paper 2005-01-2134.
[12] O. Erlandsson, "Thermodynamic simulation of HCCI engine systems," Ph.D. dissertation , Dept. Heat Power Eng., Lund Inst. Technol. , Lund Univ., Lund, Sweden, 2002.
[13] D. Popovic, M. Jankovic, S. Magner, and A. Teel, "Extremum seeking methods for optimization of variable cam timing engine operation," *IEEE Trans. Control Syst. Technol.*, vol. 14, no. 3, pp. 398–407, May 2006.
[14] K. B. Ariyur and M. Krstic, *Real-Time Optimization by Extremum Seeking Feedback*. Hoboken, NJ: Wiley-Interscience, 2003.
[15] G. Haraldsson, P. Tunestål, B. Johansson, and J. Hyvönen, "HCCI combustion phasing with closed-loop combustion control using variable compression ratio in a multi cylinder engine," 2003, SAE Paper 2003-01-1830.
[16] J. Hyvönen, G. Haraldsson, and B. Johansson, "Balancing cylinder-to-cylinder variations in a multi-cylinder VCR-HCCI engine," presented at the SAE Fuels & Lubricants Meeting & Exhibition, Toulouse, France, 2004, SAE Paper 2004-01-1897.
[17] F. Agrell, H. E. Ångstrom, B. Eriksson, J. Wikander, and J. Linderyd, "Control of HCCI during transients by aid of variable valve timings through the use of model based nonlinear compensation," 2005, SAE Paper 2005-01-0131.
[18] P. Strandh, J. Bengtsson, R. Johansson, P. Tunestål, and B. Johansson, "Cycle-to-cycle control of a dual-fuel HCCI engine," presented at the SAE 2004 World Congr. & Exhibition, Detroit, MI, 2004, SAE Paper 2004-01-0941.
[19] K. J. Åström and T. Hägglund, *PID Controllers: Theory, Design and Tuning*, 2nd ed. Research Triangle Park, NC: ISA, 1995.
[20] H. Hjalmarsson, M. Gevers, S. Gunnarsson, and O. Lequin, "Iterative feedback tuning: Theory and applications," *IEEE Control Syst. Mag.*, vol. 18, no. 4, pp. 26–41, Aug. 1998.
[21] C. C. Hernändez, "HCCI timing control using iterative feedback tuning," M.S. thesis , Dept. Elect. Eng., Royal Inst. Technol. (KTH), Stockholm, Sweden, 2006.
[22] N. J. Killingsworth and M. Krstić, "PID tuning using extremum seeking: Online, model-free performance optimization," *IEEE Control Syst. Mag.*, vol. 26, no. 1, pp. 70–79, Feb. 2006.
[23] J. Y. Choi, M. Krstic, K. B. Ariyur, and J. S. Lee, "Extremum seeking control for discrete-time systems," *IEEE Trans. Autom. Control*, vol. 47, no. 2, pp. 318–323, Feb. 2002.
[24] E.-W. Bai, L.-C. Fu, and S. Sastry, "Averaging analysis for discrete time and sampled data adaptive systems," *IEEE Trans. Circuits Syst.*, vol. 35, no. 2, pp. 137–148, Feb. 1988.
[25] Y. Tan, D. Nešić, and I. M. Y. Mareels, "On global extremum seeking in the presence of local extrema," in *Proc. 45th IEEE Conf. Decision Control*, San Diego, CA, 2006, pp. 5663–5668.
[26] E. Schuster, C. Xu, N. Torres, E. Morinaga, C. K. Allen, and M. Krstic, "Beam matching adaptive control via extremum seeking," *Nucl. Instrum. Methods Phys. Res. A, Accel. Spectrom. Detect. Assoc. Equip.*, vol. 581, no. 3, pp. 799–815, Nov. 2007.
[27] D. L. Flowers, J. Martinez-Frias, F. Espinosa-Loza, N. J. Killingsworth, S. M. Aceves, R. Dibble, M. Krstic, and A. Bining, "Development and testing of a 6-cylinder HCCI engine for distributed generation," in *Proc. ASME ICEF*, Ottawa, ON, Canada, 2005, pp. 465–473.
[28] J. Bengtsson, P. Strandh, R. Johansson, P. Tunestål, and B. Johansson, "Closed-loop combustion control of homogeneous charge compression ignition (HCCI) engine dynamics," *Int. J. Adapt. Control Signal Process.*, vol. 18, pp. 167–179, Jan. 2004.
[29] O. Lequin, M. Gevers, and T. Triest, "Optimizing the settling time with iterative feedback tuning," in *Proc. 14th IFAC World Congr.*, Beijing, China, 1999, pp. 433–437.
[30] C. J. Chiang and A. G. Stefanopoulou, "Stability analysis in homogeneous charge compression ignition HCCI engines with high dilution," *IEEE Trans. Control Syst. Technol.*, vol. 15, no. 2, pp. 209–219, Mar. 2007.

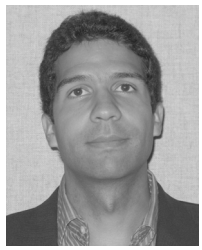

Nick J. Killingsworth (S'05–M'08) received the B.S. degree in mechanical and materials science engineering and the M.S. degree in mechanical engineering from the University of California, Davis, in 2000 and 2002, respectively, and the Ph.D. degree in mechanical engineering from the University of California, San Diego, La Jolla, in 2007.

He conducted his Ph.D. research as a SEGRF Fellow in residence at Lawrence Livermore National Laboratory, Livermore, CA, where he is currently a Postdoctoral Researcher with the Energy Conversion and Storage Group. His research interests include control of internal combustion engines, combustion instabilities, and extremum seeking.

Salvador M. Aceves received the B.S. degree in mechanical engineering from the University of Guanajuato in 1984, and the M.S. and Ph.D. degrees in mechanical engineering from Oregon State University in 1986 and 1989, respectively.

Since 1993, he has been with Lawrence Livermore National Laboratory, Livermore, CA, where he has been working on internal combustion engine analysis since 1994 and is currently the Group Leader of the Energy Conversion and Storage Group. In 1996, he started working on HCCI combustion, focusing on the development of computationally efficient analysis techniques and control strategies.

Mr. Aceves is an Associate Editor of the ASME transactions, *Journal of Energy Resources Technology*. His professional affiliations include membership in American Society of Mechanical Engineers (Fellow) and the Society of Automotive Engineers.

Daniel L. Flowers received the B.S., M.S., and Ph.D. degrees in mechanical engineering from the University of California, Davis, in 1996, 1997, and 2001, respectively.

He is currently a Mechanical Engineer with the Energy Conversion and Storage Group, Lawrence Livermore National Laboratory (LLNL), Livermore, CA. His work focuses on experimental and analytical research in thermal sciences and combustion. He has been working in the area of homogeneous-charge-compression-ignition (HCCI) engine combustion since joining LLNL in 1998, where he also lead several combustion research projects in the areas of HCCI and hydrogen and diesel combustion.

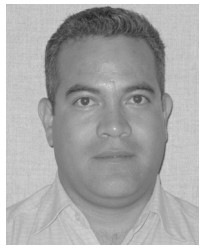

Francisco Espinosa-Loza received the B.S. and M.S. degrees in mechanical engineering from the University of Guanajuato, Guanajuato, Mexico, in 1993 and 2001, respectively. He is currently working toward the Ph.D. degree in mechanical engineering, University of California, Davis.

He is currently a Mechanical Engineer in the Laser Systems Engineering and Operations Division at Lawrence Livermore National Laboratory, Livermore, CA. His work focuses on energy conversion and hydrogen storage. He has experience with both

experimental and analytical research in thermal sciences and combustion. He has been working in the area of Homogeneous Charge Compression Ignition (HCCI) engine combustion since 2002, and hydrogen storage since 2001. From 2000 to 2001, he worked for the Combustion Center of Excellence at GE Aircraft Engines.

Miroslav Krstić (F'02) received the Dip.Ing. degree in electrical engineering from the University of Belgrade in 1989, and the M.S. and Ph.D. degrees in electrical engineering from the University of California, Santa Barbara, in 1992 and 1994, respectively.

He is currently the Sorenson Distinguished Professor with the Department of Mechanical and Aerospace Engineering and the Founding Director of the Cymer Center for Control Systems and Dynamics, University of California, San Diego. He was a Springer Visiting Professor with the University of California, Berkeley. He is the coauthor of the books *Nonlinear and Adaptive Control Design* (Hoboken, NJ: Wiley, 1995), *Stabilization of Nonlinear Uncertain Systems* (New York: Springer, 1998), *Flow Control by Feedback* (New York: Springer, 2002), *Real-time Optimization by Extremum Seeking Control* (Hoboken, NJ: 2003), *Control of Turbulent and Magnetohydrodynamic Channel Flows* (Cambridge, MA: Birkhauser, 2007), and *Boundary Control of PDEs: A Course on Backstepping Designs* (Philadelphia, PA: SIAM, 2008).

Mr. Krstić was the recipient of the Axelby, Schuck, NSF Career, ONR YI, and PECASE Awards and the UCSD Research Award. He is a Fellow of IFAC. His has also served on editorial boards of the IEEE TRANSACTIONS ON AUTOMATIC CONTROL, *Automatica*, *SCL*, and *IJACSP*. He served Control Systems Society as the Vice President for Technical Activities and Chair of the IEEE Fellow Committee.